4. EXPERIMENTAL FACILITIES IN BEAM HALL

4.1 NEUTRON DETECTOR ARRAY FACILITY

The first phase of the Neutron Detector array facility consisting of 50 detectors and associated electronics system has been installed at beam hall II of IUAC accelerator facilities. Each detector is a 5"×5" liquid scintillator of type BC501A coupled to 5" photomultiplier tube. Major work on the installation of detectors, signal cabling, beam line assembly, beam dump shielding, electronics and data acquisition has been completed. Signal processing for 50 detectors has been implemented using home-made pulse shape discrimination modules and other standard analog NIM electronics. The data acquisition setup uses VME hardware and LAMPS software. All the sub-systems of the facility have been tested for their performance for on-line measurements in a test experiment using ^{19}F beam on ^{208}Pb targets. Two multi-wire proportional counters(MWPC) have been used for detection of fission fragments at complementary angles.

4.1.1 Characterization of liquid scintillators for NAND facility

N. Saneesh[1], Meenu Takur[2], Ruchi Mahajan[2], Gurpreet Kaur[2], R. Dubey[1], S. Venkataramanan[1], A. Jhingan[1] and P. Sugathan[1]

[1]Inter University Accelerator Centre, Aruna Asaf Ali Marg, New Delhi 110067, India

[2]Department of Physics, Panjab University, Chandigarh 160014, India

All the 50 detectors used in the array have been tested offline using standard radioactive sources. The linearity of the light output from the detectors has been tested by measuring the light output for different γ-sources (^{137}Cs, ^{60}Co, ^{22}Na, etc.) and determining the corresponding Compton edges. A good linear relationship between the deposited energy and the light output has been observed. The timing performance of the detectors has been tested by a time of flight (TOF) setup measuring γ-rays in coincidence using a BaF2 detector and a liquid scintillator. A typical time spectra for coincidence γ-rays from ^{22}Na source, recorded between the two detectors, is shown in figure 1. Here, an FWHM of 1.56 ns has been observed. The neutron-γ discrimination property of the detector plus home-made pulse shape discrimination module has been tested by detecting the radiations from ^{252}Cf source. Figure 2 shows the two dimensional histogram displaying the light output plotted against the "zero cross time" distribution for one detector using neutrons and γradiations from ^{252}Cf source. Distinct separation between neutron and γ events from the source is clearly visible, illustrating the performance of the pulse shape discrimination of the setup. The figure of merit (FOM), defined as the ratio of peak separation to the sum of full width at half maximum (FWHM) of the peaks is found to be 1.62 at 120keV recoil electron energy. Neutron-γ discrimination at thresholds in the range between 250 and 500 keVeehave been found for all the 50 detectors tested. These threshold values are good enough for most of the reaction-mechanism studies.

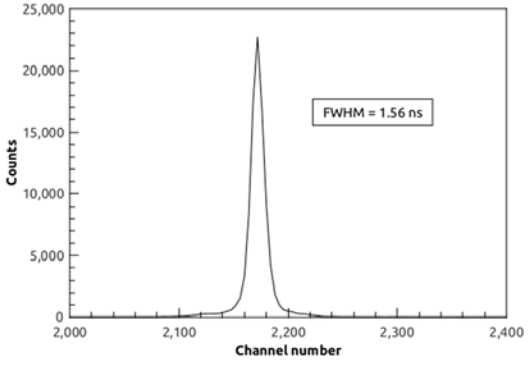

Fig. 1.Time of flight spectrum of γ-rays from ^{22}Na having FWHM of 1.56 ns.

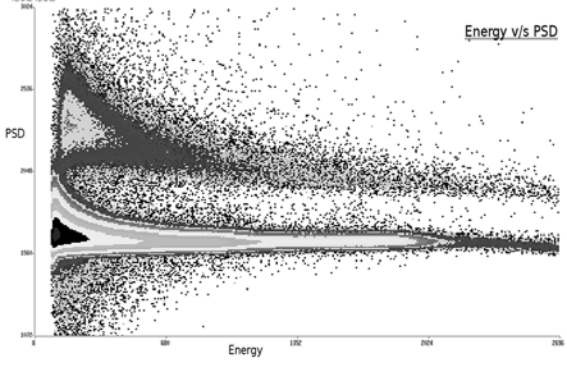

Fig. 2. Neutron-γ discrimination using home-made PSD module based on zero-cross timing.

4.1.2 Design, fabrication and testing of fast neutron shielding blocks for NAND

N. Saneesh, S.K. Saini, S. Rao, A. Jhingan and P. Sugathan

In the NAND beam-line, the ion beam passing through the reaction target is stopped beyond the detector array in a beam dump located 4 m downstream from the target. This can initiate secondary radiations including fast neutrons from the dump. In order to limit these background radiations reaching the neutron detectors, proper shielding of the beam dump has been built using borated paraffin blocks and lead sheets surrounding the dump. To evaluate the neutron shielding effect on various materials, a detailed analysis of the material composition and the geometry has been performed by a Monte-Carlo simulation using FLUKA particle transport and interaction code. The optimum composition of the shielding material has been chosen to be 70% (mass fraction) of paraffin wax mixed with 30% of boric acid.The overall dimensions of the shielding blocks are 120(l) × 80(h) × 80(w) cm3. The blocks have been fabricated at IUAC workshop by melting and mixing the composition of paraffin and boric acid powders under temperature controlled environment. The effectiveness of these borated paraffin blocks in neutron shielding has been tested in an off-line experiment measuring neutron energy from ^{252}Cf source by time of flight method. Figure 3 shows the TOF spectrum where neutrons are well separated from γ-rays. In Figure 4, the TOF spectrum is shown when 40 cm thick borated paraffin block is introduced between the source and the neutron detector. Absence of the peak corresponding to neutrons shows effective shielding of fast neutrons by the borated paraffin block.

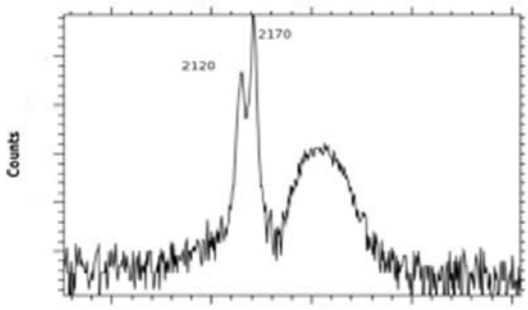

Fig. 3. Time of flight spectrum of neutrons and γ-rays.

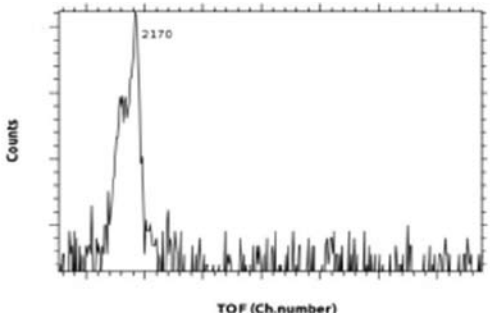

Fig. 4 TOF spectrum with a 40 cm thick borated paraffin block introduced between the source and the neutron detector.

4.1.3 Beam test of NAND facility

P. Sugathan[1], A. Jhingan[1], N. Saneesh[1], G. Mohanto[1], D.Siwal[1], R. Dubey[1], T. Banerjee[1], Gurpreet Kaur[2], M.Thakur[2], R.Mahajan[2], P.Sharma[2], K.Kapoor[2], B. R. Behera[2], N.Kumar[3], Kushboo[3], S.Goel[3], M. Shareef [4] and H. Singh[5]

[1]Inter University Accelerator Centre, Aruna Asaf Ali Marg, New Delhi 110067, India

[2]Department of Physics, Panjab University, Chandigarh 160014, India

[3]Department of Physics and Astrophysics, Delhi University, Delhi 110007, India

[4]Department of Physics, Central University of Kerala, Kasaragod, Kerala 671328, India

[5]Department of Physics,Kurukshetra University, Kurukshetra, Haryana136119, India

In December 2013, we performed a facility test in the neutron detector array using ^{19}F beam on ^{208}Pb target. The pulsed beam from Pelletron at E_{lab} = 110MeV was used to bombard ~600μg/cm^2 lead target and neutrons were detected in all 50 detectors. Two multi-wire proportional counters(MWPC) were mounted inside the 1m diameter spherical vacuum chamber. The MWPCs, kept at folding angles, detected the fission fragments. Two silicon detectors were used to monitor the beam. All the signals, routed to the new data room, were processed using custom made electronics. The master

trigger was generated from a coincidence between the beam RF and any of the fission detector signals and vetoed by the common busy of the data acquisition. The VME based data acquisition using LAMPS software was used to acquire and store event mode data. The facility test was used to check signals from all detectors, beam alignment, target ladder control, vacuum system, beam dump, electronics and data acquisitions systems. Signals from all the detectors were used for tuning various parameters of the setup. The operational pressure obtained in the scattering chamber was ~4×10^{-6} Torr with two MWPC detectors operating at 2 Torr pressure of iso-butane gas. Custom made fast electronics for the MWPC signal readout were also placed inside the chamber. The data acquisition was performed on single crate VME system with more than 200 parameters. In Figure 5, the time of flight spectrum from the forward MWPC detector is shown. Events corresponding to various reaction products are clearly separated by distinct peaks on the TOF spectrum. A two dimensional histogram, showing PSD vs TOF from one of the neutron detectors, is given in Figure 6. Neutrons from the fission products are distinctly separated from the γ background.The TOF information is used for determining the energy of the neutrons.

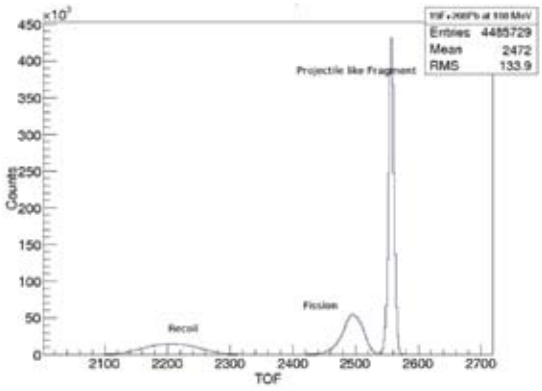

Fig 5. TOF spectrum from the forward MWPC.

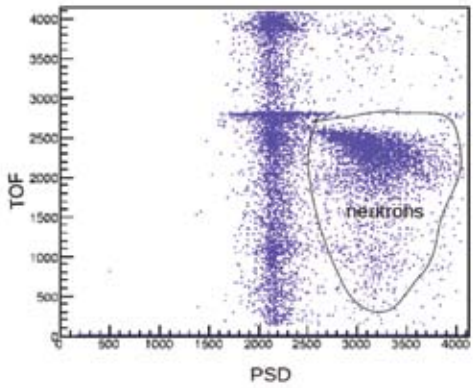

Fig 6. PSD vs TOF spectrum from one of the neutron detectors.

4.2 GAMMA DETECTOR ARRAY

R.K. Gurjar, Indu Bala, Kusum Rani, B. Kumar, S.K. Saini, M.Kumar Raju, R.Kumar, A. Jhingan, S. Muralithar and R.P. Singh

4.2.1 Upgradation of GDA setup

A new support structure was designed for mounting 18 Compton-suppressed Clover high purity germanium detectors in the GDA beam line in beam hall I. The schematic picture of the structure is shown in figure 7.

The new structure can support 4 Clover detectors with their Anti-Compton Shields (ACS) at 148°, 2 at 123°, 6 at 90°, 2 at 57° and 4 at 32° with respect to the beam

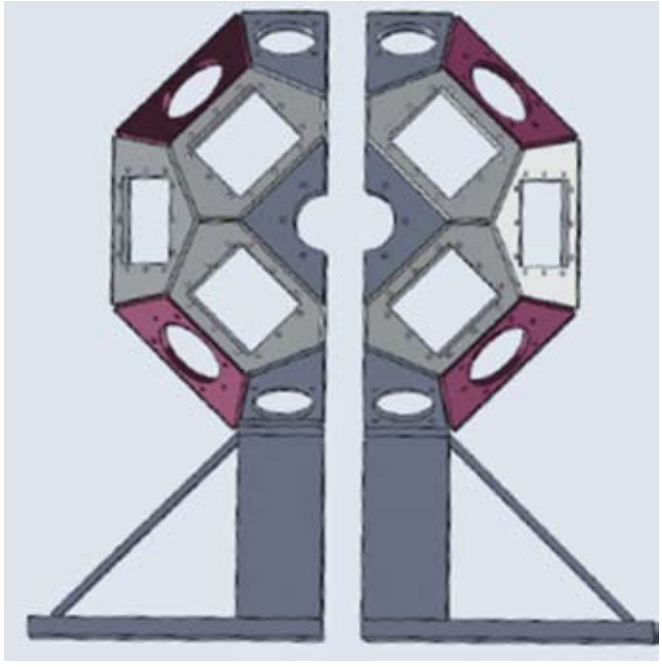

Fig. 7. Schematic drawing of the new GDA support structure.

direction. The structure can also support up to 8 Low Energy Photons (LEPS) detectors along with BGO detector array for multiplicity measurements. The distance of each Clover detector figure 5 from the target, stopper center is about 24 cm. There will be inner space of about 20 cm, in diameter, in the fully closed configuration of the array. The support structure will be mounted on precision guide rails with motorised drives. A card board model of the structure was also made in the laboratory.

The array is designed with enough flexibility to couple different ancillary devices like a Charge Particle Detector Array (CPDA), Plunger and PPAC for Coulex studies. There are also scopes for γ–ray spectroscopy of fission fragments and transient field g-factor measurements. The extension of the beam line for the Perturbed Angular Distribution (PAD) setup will be unaltered.

4.2.2 Plunger Device for INGA

The new plunger device, shown in figure 8, was developed for lifetime measurements of excited nuclear states in the sub-nanosecond range with the Indian National Gamma Array (INGA). The device consists of 3 DC micro-motors for precision motion of the target foil. Three motors of the first batch had developed technical snag and were sent to the factory for repair. The device is now again being tested in the laboratory for distance measurements and is ready for experiments with INGA.

Fig. 8. Plunger device for INGA, reassembled with new DC micro-motors.

4.2.3 Plunger set-up in GDA

The old plunger device had not been used for a long time. This device was overhauled; the coupling springs were changed and the support rods were polished. Electrical connections for the target,stopper, collimator and the Faraday cup were re-done. Fig. 9(a) and 9(b) show the plunger assembled in the GDA setup. A test experiment followed by an experiment by a Delhi university group was carried out.

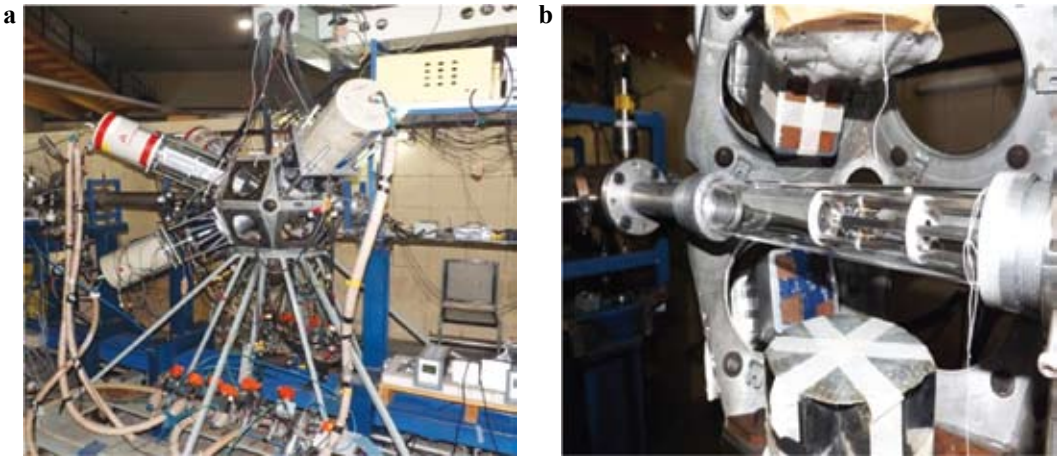

Fig. 9. (a) Plunger in the GDA setup and (b) inside view of the plunger during test experiment.

4.2.4 Repair of Clover and HPGe detectors

A clean room with necessary infrastructure was set-up for repair of high purity germanium detectors. Four Clover detectors were serviced with engineers from Canberra, France. Servicing of detectors in our laboratory provided opportunity for training our personnel and people from other institutes. Figure 10a shows a picture taken at the time of repair of a clover detector.

Fig. 10a: A Clover detector being repaired

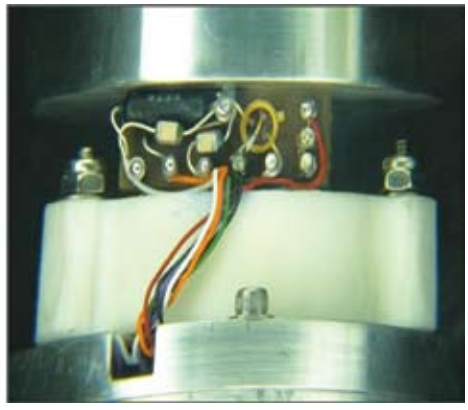

Fig.10b: A FET replaced in a HPGe detector.

One faulty FET was replaced by our engineer in one of the old HPGe detectors. The detector was found to work properly after the replacement. The new FET, mounted in the detector, is shown in the figure 10b.

4.2.5 Setup for study of nuclei through Coulomb excitation in GDA

A set-up consisting of a Parallel Plate Avalanche Counter (PPAC) in conjunction with four Clover detectors was made for study of nuclei through Coulomb excitation. The γ-rays were collected in coincidence with the scattered ions is the position sensitive PPAC detector. Figure 11 shows a picture of the setup in GDA.

Fig. 11. A large area PPAC with four Clover detectors mounted on GDA structure.

4.2.6. Augmentation of BGO multiplicity filter array

We have acquired 15 more BGO detectors with hexagonal crystals each of size ~40 mm (vertex-vertex) × 75 mm (length) to augment the efficiency of our multiplicity filter array. This could also be used with the INGA array as a multiplicity and energy sum spectrometer. Figure 12 shows the spectra for 661 keV γ-ray peak obtained with these BGO detectors.

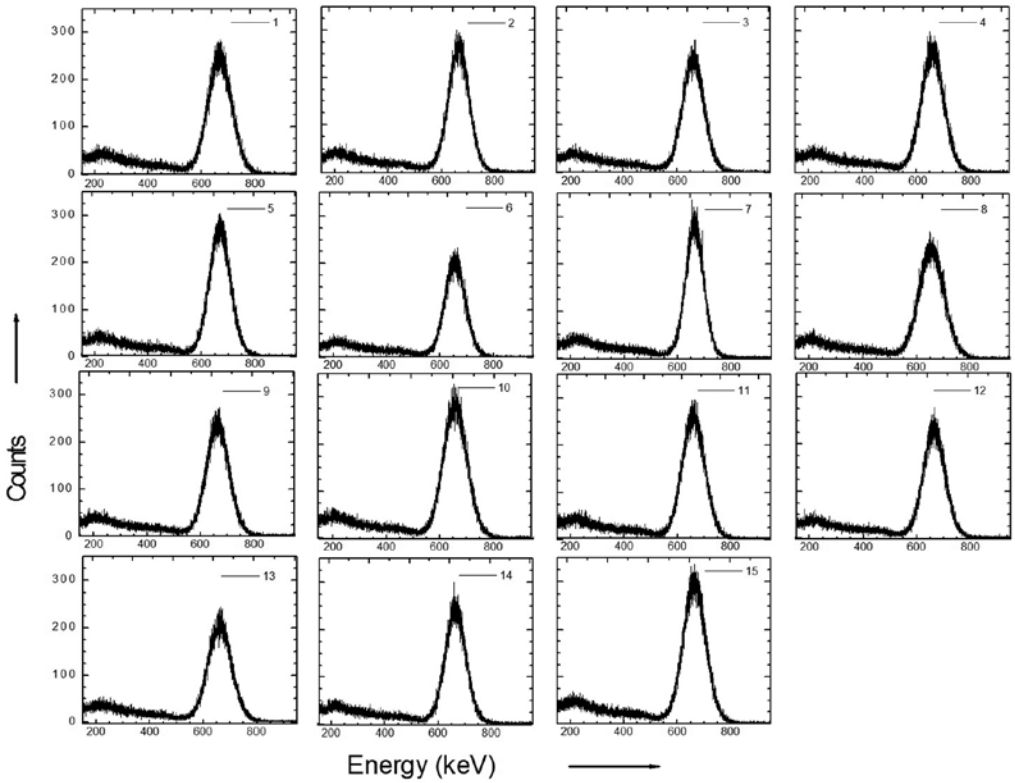

Fig. 12: Spectra obtained from 15 BGO detectors for 661 keV γ-ray from ^{137}Cs.

4.2.7 Test of CSI (Tl) detector

For the planned Charge Particle Detector Array (CPDA) for INGA, a CsI(Tl) crystals each of size 20 mm × 20 mm and thickness 3 mm was coupled to a photo diode (10 mm × 10 mm).The detector was tested for energy resolution for α-particles from ^{241}Am. The shaping time used for the 572 ORTEC amplifier was 3 μs. The spectrum obtained is shown in figure 13. Energy resolution was observed to be 5% with 30V bias voltage.

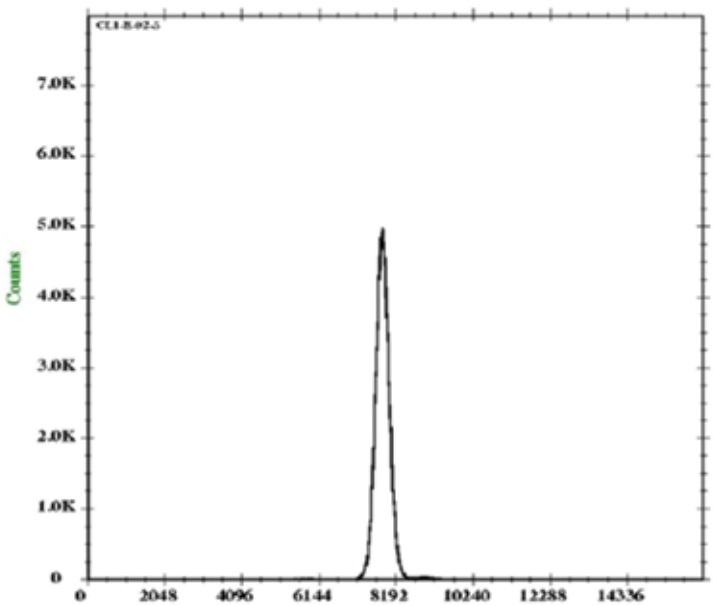

Fig.13 : Energy spectrum of 5.486 MeV α-particles from ^{241}Am source.

4.2.8 Recent experiments carried out in GDA

- Study of entrance channel effects on incomplete fusion dynamics in heavy ion induced reactions at E= 3-7 MeV/nucleon,
- Nuclear electromagnetic moment measurements in the A~130 mass region using PAD setup,
- Coulomb excitation of ^{120,122,124}Te and
- Lifetime measurements in ^{102}Pd using plunger setup.

4.3 RECOIL MASS SPECTROMETERS (HIRA AND HYRA)

S. Nath, J. Gehlot, T. Varughese, A. Jhingan and N. Madhavan

Heavy Ion Reaction Analyzer (HIRA) was used in a student thesis experiment to perform angular distributions of Evaporation Residues (ERs) and for the experimental determination of ER transmission efficiency through HIRA for an asymmetric and a nearly symmetric system, both leading to same compound nucleus (CN) in similar excitation energy range. This was a continuation of an earlier experiment which measured the average angular momentum of ERs in those two systems.

The 4π TIFR spin spectrometer set up at the target site of HYRA was used in conjunction with HIGRASP setup for spin gated Giant Dipole Resonance (GDR) decay in hot, rotating heavy nucleus. This too was a continuation of an earlier experiment for better statistics and angular distribution studies.

The superconducting quadrupole doublet (SC Q1-Q2), being developed primarily by Cryogenics group at IUAC, has been finally welded in-house after assembly. Initial tests showed that a field value of close to 2.0 T at 10 cm radius is attainable using the 100 A power supply. Tests were carried out up to 75 A. The deviation of magnetic axis from the geometric axis was corrected in the vertical direction. However, the horizontal correction and detailed field mapping are yet to be carried out. The two cryo-coolers could maintain the topped up liquid Helium level at more than 85% level for more than a month.

The SC Q1-Q2, which will be the first electromagnetic component of HYRA, is crucial for commissioning the second part of HYRA as a quadrupole doublet from the second stage is being used in the first stage temporarily. Based on the above mentioned progress in the development of SC Q1-Q2, the setting up of second stage of HYRA has been taken up (Fig. 14). The electrode assembly was set up in a clean enclosure (Fig. 15) and aligned with respect to each other (Fig. 16). Subsequently, the ED set-up has been placed in the already aligned ED chamber (Fig. 17). The quadrupole doublet Q6-Q7 has also been aligned. Q6-Q7 also have the sideways movement capability (Fig. 18), similar to Q3 split quadrupole, in order to accommodate more detectors at the first stage focal plane, in future.

Fig. 14 Electromagnetic components of HYRA second stage

Fig. 15 The electrodes of ED (HYRA) set up in a clean room

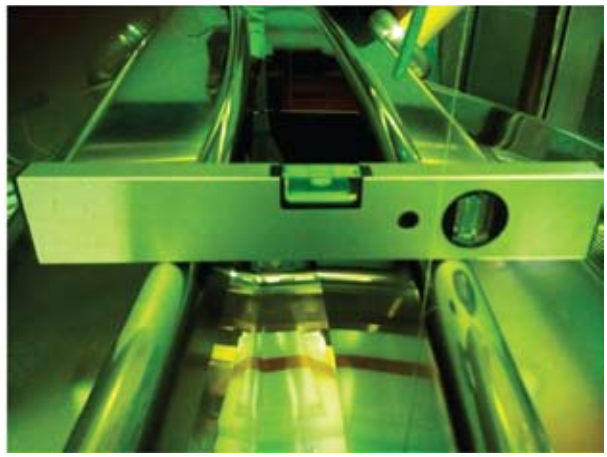

Fig. 16 The electrodes of ED (HYRA) aligned with respect to each other with a gap of 120 mm

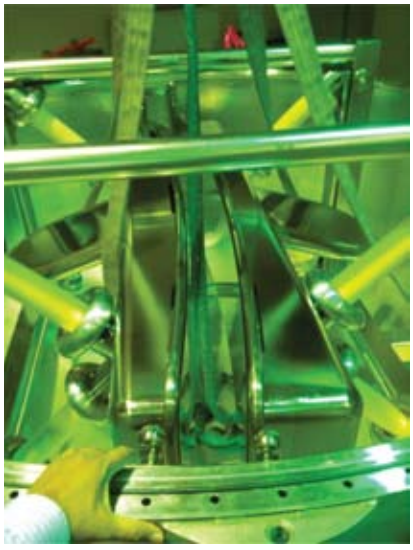

Fig. 17 The ED set up placed in the ED chamber after alignment of electrodes w.r.t. each other

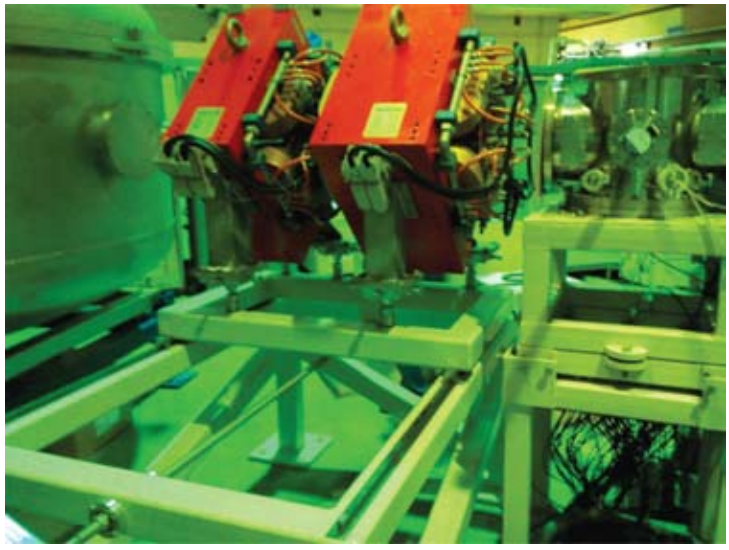

Fig. 18 Aligned Q6-Q7 set up (option for sideways movement is seen)

A compact aluminium chamber with large exit port, to match with the acceptance of HYRA, has been fabricated and installed. This can be used in conjunction with arrays such as TIFR 4π spin spectrometer (presently coupled to HYRA) and INGA (planned to be coupled to HYRA).

4.4 MATERIALS SCIENCE FACILITY

A. Tripathi, K. Asokan, V.V. Sivakumar, Fouran Singh, S.A. Khan, P. K. Kulriya, I. Sulania, P. Barua, A. Kothari and D.K. Avasthi

The materials science facilities continue to support the research programmes of a large number of users from different universities and institutions. This year there have been a total of 56 user experiments in materials science beamline with energetic ion beams. These were spread over 175 shifts and were performed without any major beam time loss due to facility break down. Out of these 23 runs were BTA experiments associated with students' Ph.D. programmes. The swift heavy ion (SHI) irradiation and related experiments are mostly performed in the irradiation chamber in the materials science beamlines in beamhall-I, though 2 experiment running over 12 shifts were performed in materials science beamline

in beamhall-II. Experiments are being done in different areas of SHI induced materials modification and characterization and the details of the research programmes are given in Section 5.2.

The materials synthesis techniques: RF sputtering system, microwave plasma system, ball milling system, box furnace and tubular furnaces are being extensively used by users for preparing samples. The off-line characterization facilities: XRD, UV-Vis, SPM, SEM, micro-Raman and transport measurement facilities continue to be used by a large number of users.

4.4.1 Irradiation chamber maintenance

S A Khan, P Barua and A. Tripathi

The irradiation chamber in materials science beamline was used in more than 164 shifts of irradiation experiments from 54 users. The system has been running without any problem.

A facility test was taken to optimize the ERDA setup for use with 120 MeV Ag ions. The setup for simultaneous hydrogen (by SSBD) and heavier recoils by telescope detector was tested for this purpose. The gas pressure and voltages were optimized for the telescope detector. Simultaneous recording of charge collected from the ladder during measurement was incorporated. The computer system has also been upgraded for the setup.

4.4.2 Scanning Probe Microscope

I.Sulania, Sunil Kumar and A. Tripathi

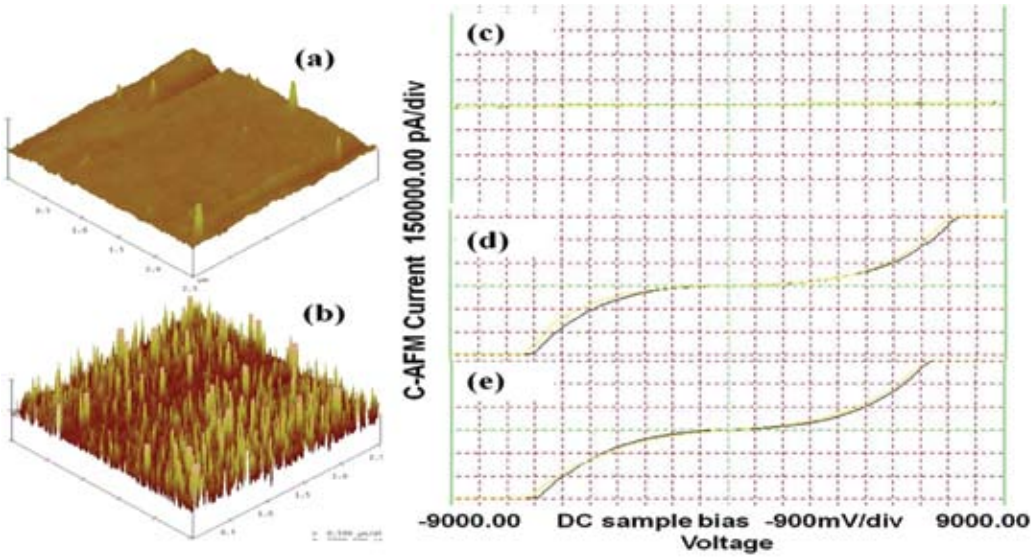

Fig. 19. The topographic (a) and current (b) image using C-AFM shows formation of conducting tracks in the sample after irradiation. The IV measurements show increased conductivity in samples with 5% (d) and 10% Ag doping (e) as compared to unirradiated sample (c).

Last year about 600 samples have been scanned; 470 in tapping mode, 100 samples in MFM mode, besides about 30 samples in C-AFM mode.

There was a software breakdown problem while trying to load CAFM software. The problem was detected with the fan of the CPU on the motherboard. The problem was rectified by changing the fan of the motherboard.

The formation of conducting tracks in thin films of C_{60} and silver co-deposited film as a result of ion bombardment was studied. The current image of the sample and I-V measurement on the conducting part is shown in Figure 19.

4.4.3 Field emission scanning electron microscope (FE-SEM)

A. Tripathi, S.A. Khan and Sunil Kumar

The field emission scanning electron microscope (FE-SEM) from TESCAN, MIRA II LMH CS is regularly being used to boost research activities in nanomaterials and other systems. This year the system has been used for studying surface morphology of nearly 430 samples from 96 users besides elemental analysis of 270 samples from 30 users in EDS mode. The sputter coater was used to provide conductive coatings of gold and carbon for better imaging of nearly 230 insulating samples from 56 users. More than 30 samples were imaged in cross-sectional mode.

The UPS power related problems, which resulted in 3 breakdowns last year were solved and the system had smooth operation. The FE source has run for more than four years and its tuning was also undertaken. There were a few software problems but they could be simply solved by re-setting the system.

The SEM images of Graphene samples (CVD grown graphene on Ni/SiO_2) which were coated with Au of 1.2 nm film thicknesses and annealed at 400ºC for the formation of Au nanoparticles on graphene are shown below.

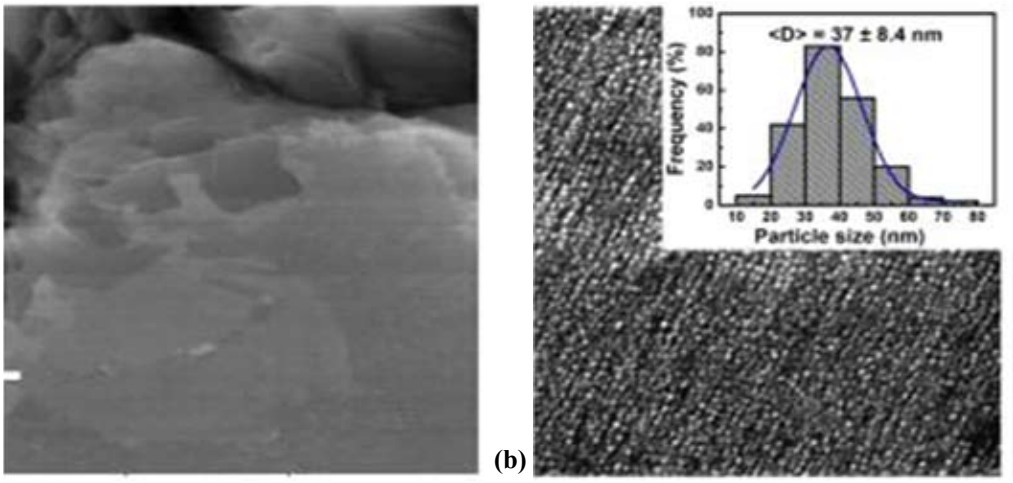

Fig. 20 SEM images showing (a) pristine (b)1.2 nm Au, graphene samples annealed in Ar at 400ºC. (From Compesh et al, Appl. Surf. Sc. (2014).

4.4.4 In-situ X-ray Diffractometer

P. Kulriya

The XRD lab is used by the most of user for characterization of their samples in the (a) off-line XRD (temperature varying from 20 K to 300 K) of the pristine and post irradiated sample, and (b) *in-situ* XRD for ion irradiation induced phase transformation. This year XRD system has been used for characterization of around 525 samples in the off-line XRD mode. Most of the samples are either in thin films or nanoparticle form where slow scan is required to get good statistics

In one of the highlights for offline XRD results, we have investigated the effect of temperature and pressure on hydrogen induced lattice parameter variation in size selected Pd-Ag and Pd-Cu nanoparticles. In the range of temperature (350 K to 250 K) and pressure (10^{-4} to 100 mbar), no α (H/Pd ≤0.03)↔β(H/Pd ≥0.54) phase transition is observed which have advantage of using Pd-alloy nanoparticles in applications requiring long term and repeated hydrogen cycling. These results are published in Journal of Applied Physics 115 (2014)114308 and Appl. Phys. Lett. 103 (2013) 173107. The structure studies of the TiO_2 thin films deposited by electron beam evaporation technique and annealed in O2 or Ar atmosphere is done to investigate the origin of the ferromagnetism at room

temperature. Detailed results are published in the Journal of Magnetism and Magnetic Materials 355(2014)240–245.

4.4.4.1 Up-gradation and maintenance in the facility

There was no major breakdown in the XRD system this year. Some regular maintenance and break down maintenance work is carried out in the XRD system as and when necessary. The maintenance works which routinely carried out are (a) alignment of the x-ray diffractometer (b) cleaning of the x-ray tube water filter, (c) changing water of the chiller, (d) cleaning tank of chiller, and (e) cleaning the gobble mirror etc. In addition to regular maintenance work, following repairing/up-gradation work is also done.

(a) Replacement of water chiller: The old water chiller was creating problem regularly so it is replaced with a new water chiller. The work related to installation of chiller is done.

(b) Repairing of the temperature controller and heating element is closed cycle refrigerator

(c) Problem in the Ventec-1 detector: The problem is even not rectified by service engineer. Therefore, detector is send to the factory for the repairing.

4.4.4.2 Modification in beam line between XRD chamber and high vacuum chamber

Some modification in beam line between XRD chamber and high vacuum chamber is done to make it user friendly. After modification, it has following advantages: (a) increase in the 2q range for the GAXRD, (b) reduce the risk for damage of X-ray tube, detector and CCR due to upward and downward moments of the vacuum chamber, and (c) creation of some space between XRD and high chamber which is being used for installation of gas sensing setup. Following work has been done (a) removing the exiting bellow and beam pipe, (b) installation of beam line stand, (c) cutting of the beam pipe, (d) fabrication and installation of edge welded bellow, and (e) leak testing of all the components and beam line etc.

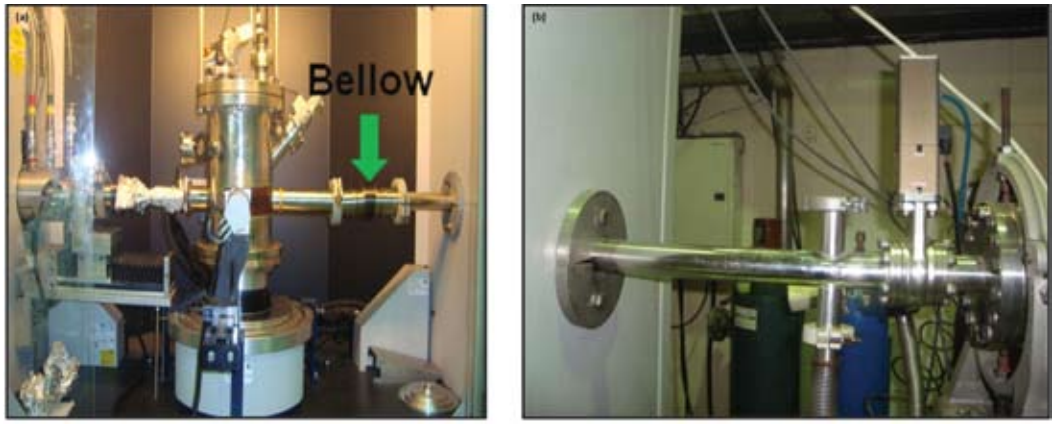

Fig. 21: Photographs of beamline after modification (a) inside, and (b) outside the XRD chamber

4.4.5 In-situ high temperature irradiation facility

P. Kulriya

The *in-situ* high temperature ion irradiation facility has been installed in the high vacuum chamber in the materials science beam line (BHII) last year. This year, we have purchased another set of heaters and temperature controllers from the BRNS project. The installation and testing of these was done. The facility has been used to investigate the radiation stability of the pyrochlore ($Gd_2Ti_2O_7$

and $Gd_2Zr_2O_7$) and CeO_2 under ion irradiation at high temperature. For example, $Gd_2Zr_2O_7$ which is readily amorphized at an ion fluence $5x10^{13}$ ions/cm^2 on irradiation with 120MeV Au ions at 300 K, whereas it is transformed to a radiation-resistant anion-deficient fluorite structure on high temperature(1000 K) irradiation, retain its crystalline nature even at ion fluence of $5x10^{13}$ ions/cm^2. The temperature dependent ion irradiation studies showed that the ion fluence required to cause amorphization at 1000 K irradiation is significantly higher than that required at room temperature irradiation. Therefore, present study establishes that the radiation stability of the pyrochlore is enhanced at higher temperatures.

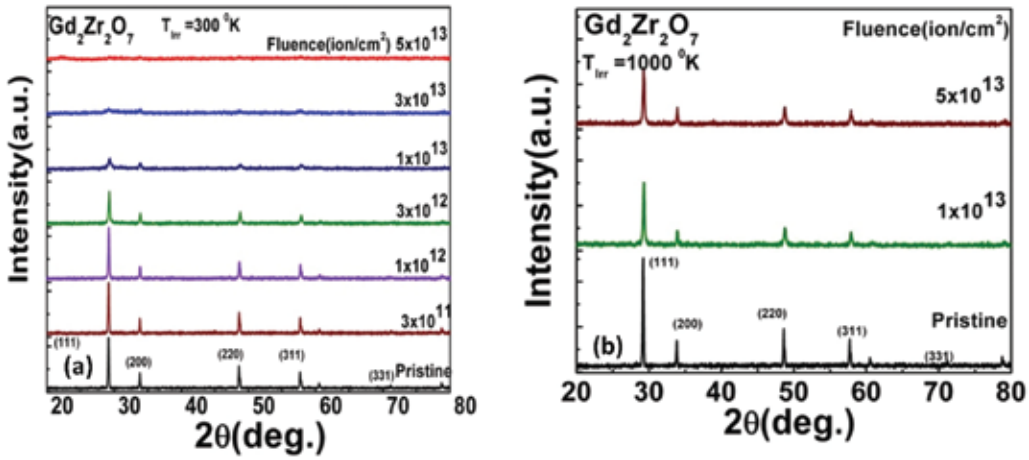

Fig. 22: Diffraction pattern of $Gd_2Zr_2O_7$ as function of Au ion fluence, recorded in the mode (a) irradiation at 300 K simultaneous *in-situ* diffraction and (b) irradiation at 1000 K – investigated using offline XRD.

4.4.6 Spectroscopy facilities and in situ testing of micro-Raman facility in beam hall with preliminary results

Fouran Singh, Subodh K. Gautam, I. Sulania, S K Saini, S. Rao, M. Archunan, and P. Barua

Spectroscopy facilities at Materials science include micro-Raman (mR), Photoluminescence (PL), ionoluminescence (IL) and Fourier Transform infrared (FTIR) facilities. mR remains heavily used facility and have served a large number users from various universities and institutes. Series of successful experiments were conducted on oxide semiconductors, graphene, ferrites and other pervoskites including multiferroics etc. The facility is in operation. Preliminary testing of this facility is also carried for its use as *in-situ* characterization of materials during the swift heavy ion (SHI) irradiation in beam hall-II. However, a detailed testing is in plan and will be carrying out soon. PL facility is in operation only for blue (441.6 nm) excitations as the life of the UV (325nm) is over. Therefore, new HeCd laser is ordered and soon UVPL will also be operational for regular experiments. A series of successful IL experiments were carried mainly for the users from Bangalore and Allahabad universities. FTIR is under maintenance, since the beam splitter has gone bad. Efforts are on the way to make it operational as soon as possible.

4.4.7 Facilities for electrical characterization of materials

Pawan Kumar, Shammi Verma, Ashish Kumar, K. Phaneendra, K. Asokan

A semiconductor device analyzer (Model B1500A) from Agilent Technologies was acquired and is now available for on-line or Off-Line characterization of semiconductor materials and devices. It provides wide range of device characterization capability with efficient and repeatable measurement. It supports all state of the art measurements (IV, CV, and fast pulsed IV), giving it the ability to cover the electrical characterization and evaluation of devices, materials, semiconductors, active/ passive components, or any other type of electronic device.

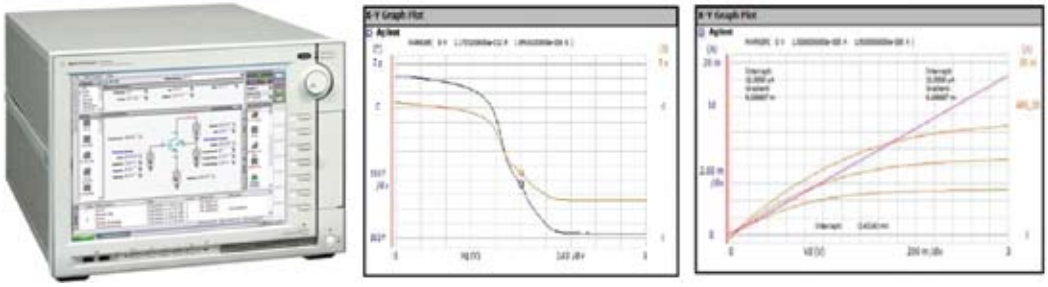

Fig. 23 (Left) Semi Conductor device analyser, (Centre & Right) Typical Graphs for CV & IV

The lab also has a Hall Effect measurement system (Model No: HMS-3000) from ECOPIA, Taiwan. It can be used for measurement at 77 K and room temperature. Besides this one can do dielectric measurements (frequency range: 20Hz-3GHz), resistivity and 1/f noise measurement facility from temperature range 77-450K. Apart from this, we are in the process of setup of high temperature (upto 700K) dielectric & resistivity measurement. Beside this a DLTS setup will be operated soon.

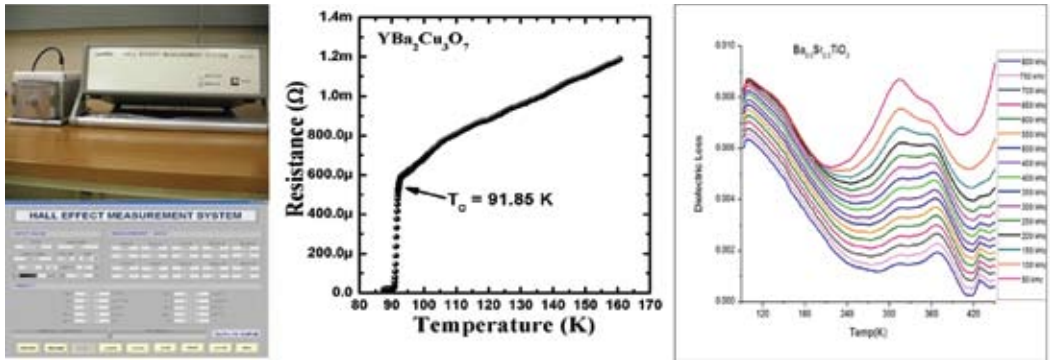

Fig. 24 (Left) Hall Effect measurement, (Center) R-T measurement, (Right) Dielectric Graph

4.4.7.1 Facilities for synthesis of samples

A sample synthesis facility with two hydraulic presses for making pellets, spin coater and spray pyrolysis for thin film preparation is available in the lab. Other facilities include two Nabertherm box furnaces (1600ºC & 1400ºC) and one tubular furnace with facility for gas flow (1400ºC).

4.4.7.2 An experimental setup for the measurement of magnetic AC-susceptibility from 10 K-325 K

T.S. Tripathi, K. Phaneendra, K. Asokan

An experimental setup has been designed for the measurement of magnetic AC-susceptibility in the temperature range 10 K – 325 K for an exchange gas closed cycle refrigerator (CCR) system. The setup consists of two secondary coils (pick up coils) connected in series opposition and a primary coil (excitation coil) for applying the low ac magnetic field. Primary coil has been kept inside the secondary coils to avoid the coupling of magnetic field from the walls of the cooling chamber.

The designing part can be classified in three sections: Cryostat, Coil assembly, Sample holder and Electronic circuit. The dimensions of our coils are as follows:

Primary coil: Length = 70 mm, Diameter = 8 mm and number of turns = 550, American Wire Gauge (AWG) 36. *Secondary coils:* Length = 10 mm, Diameter = 10 mm and number of turns = 3600 each, AWG 44 and *Biasing coil:* Length = 70 mm, Diameter = 10 mm and number of turns = 280, AWG 24 *Separation between the secondary coils:* 8 mm.

The sample holder is fabricated from a long (550 mm), thin perspecs tube of outer diameter 6 mm. At one end of this tube, a cylindrical ceramic heater (25 watt) of length 60 mm and OD 4.5 mm is attached using Araldite adhesive paste to hold the sample. Around 5 mm of the length of this ceramic heater is rubbed and made flat with the help of a diamond file. Samples in the form of thin pellets (4 mm x 4 mm x 1 mm), are glued over flat portion of the heater for measurement. A Chromega-Constantan type E thermocouple is kept in direct contact with the sample to measure its temperature. The thermocouple wires and heater wires are taken out from the other end of the perspecs tube.

Calibration and Results

For the calibration of the susceptometer, standard known samples viz. Gd_2O_3, or $MnCl_2.4H_2O$ are measured, and by comparing the measured value of the signal with the calculated value of the susceptibility for that sample, the calibration constant can be determined. For any paramagnetic sample the molar susceptibility

$$\chi_m = \frac{N_A.\mu_{eff}^2}{3k_B.T} = C_m/T$$

where, $C_m=0.125.p^2_{eff}$, $N_A = 6.022x10^{23}$, $k_B = 1.38 \times 10^{-16}$ erg/K and p_{eff} for Mn = 5.92. So, we can calculate C_m = 4.38 emu-K/mole. The value of χ_m(= Cm/T) at room temperature (T = 300 K) for $MnCl_2.4H_2O$, is then χm = 4.38/300 = 1.46x10-2 emu/mole. The calibration constant (C.C.) can be determined by using the following equation.

$$\chi_m = \frac{Signal(\mu V).Calibration\ Constant\left(\frac{emu}{\mu V}\right).Molecular\ Weight(gm)}{Sample\ Mass(gm)}$$

If the value of the signal is 10 μV for 100 mg $MnCl_2.4H_2O$ (M.W. = 196 gm) sample, the value of the calibration constant is found to be $7.45x10^{-6}$ emu/V.

This calibration constant is valid for given amplitude of primary current (i.e. rms magnetic field) and for a certain value of the frequency, which in our case were kept as 1 mA rms and 72.23 Hz, respectively. AC susceptibility data for the paramagnetic salt $MnCl_2.4H_2O$, Gd_2O_3 is shown in figure 25.

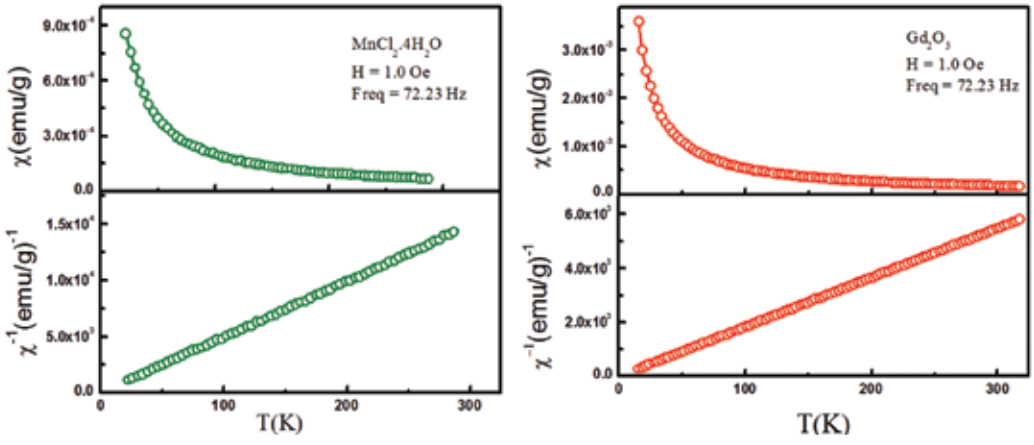

Fig. 25 AC susceptibility data of (Left) $MnCl_2.4H_2O$, & (Right) Gd_2O_3

4.4.7.3 An experimental setup for the simultaneous measurement of thermoelectric power of two samples from 77 K - 500 K

T.S. Tripathi, Manju Bala, K. Asokan

An experimental setup for the simultaneous measurement of the thermoelectric power (TEP) of two samples in the temperature range from 77K to 500K using optimum electtronic instruments. The setup consists of two rectangular copper bars in a bridge arrangement for sample mounting, two surface mount (SM) chip resistors for creating alternate temperature gradient and a type E thermocouple in differential geometry for gradient temperature (ΔT) measurement across the samples. In addition, a diode arrangement has been made for the alternate heating of SM resistors using only one DC current source. The measurement accuracy of ΔT increases with the differential arrangement. For the calibration of the setup, measurement of S on a high purity (99.99%) platinum wire and type K thermocouple wires Chromel and Alumel have been performed from 77 K - 500 K with respect to copper lead wires.

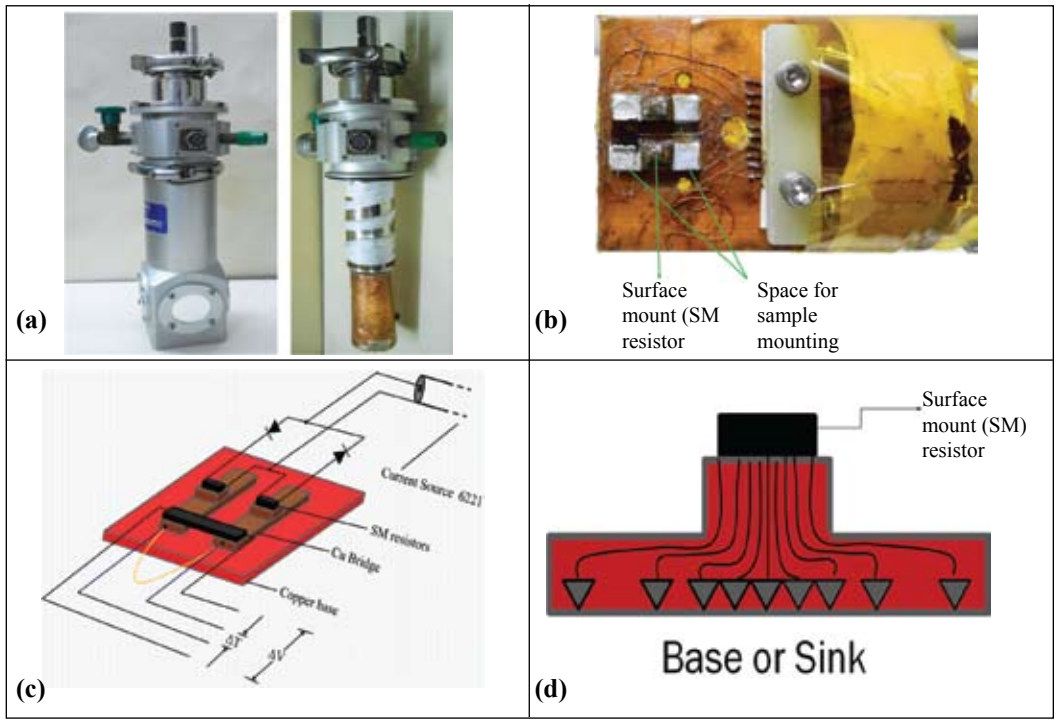

Fig. 26 Schematic Diagram of TEP

4.4.8 Plasma based systems for thin film deposition.

V.V. Siva Kumar.

The rf sputtering system was operational and used for thin film depositions of users. Some of the targets used for thin films deposition for ion beam irradiation experiments are Galfinol, Fe doped SnO_2, TiO_2, SnO_2, MgxZn1-xO, SiO_2, Al_2O_3, PbS, $Fe_{40}Ni_{38}Mo_4B_{18}$ and Zinc Ferrite. A total of 240 thin films were grown with these targets for user research works.

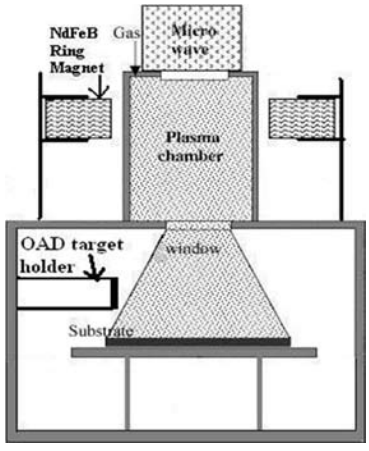

Fig 27. Schematic of ECR CVD/ OAD system showing the clamp arrangement for the NdFeB magnet.

The bottom plate of the deposition chamber of rf sputtering system was modified to improve the high vacuum to 10^{-6} torr range. A high vacuum of 5 x 10^{-6} torr vacuum was obtained after the modifications.

In the microwave/ECR plasma system, the ECR plasma chamber was fabricated for TE_{112} excitation. The NdFeB ring magnet was fixed on the chamber wall using a clamp arrangement (Figs 27, 28a). The single ring magnet produced the required 875 gauss magnetic field inside the plasma chamber and the magnetic field decreased towards the substrate holder, i.e a divergent magnetic field was produced. The magnetic field strength was measured using a gauss meter. The system was successfully tested by producing ECR argon plasma in the plasma chamber by applying a microwave power of 200 watts at 50 mtorr process pressure and adjusting the 3 stub tuner. The ECR plasma flowed from the plasma chamber to the deposition chamber due to the pressure gradient and the divergent magnetic field (Fig 28b).

(a) (b)

Fig. 28. (a) TE_{112} plasma chamber with the NdFeB magnet and (b) ECR argon plasma produced in the plasma chamber.

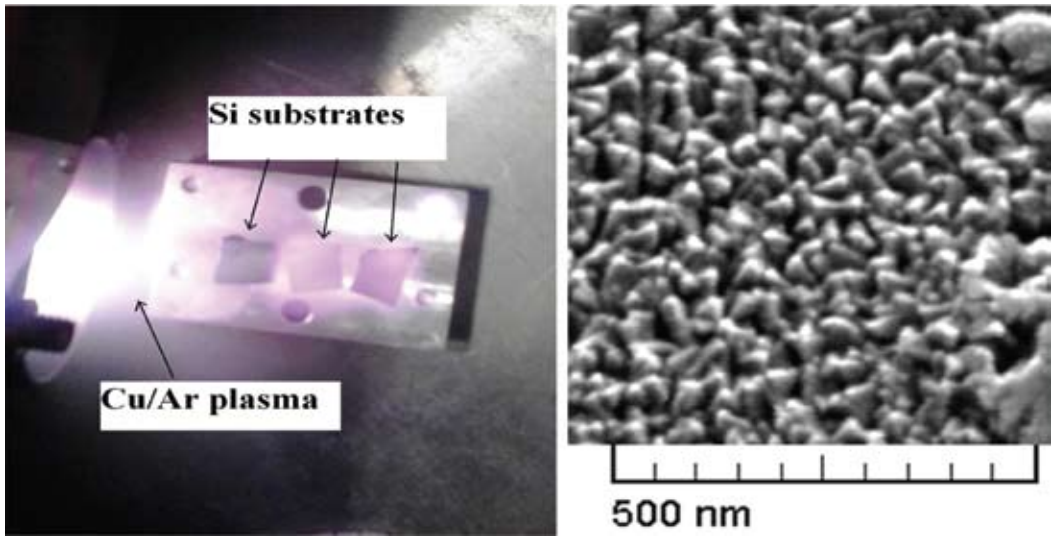

(a) (b)

Fig. 29. (a) Cu/Ar dc plasma for OAD, and (b) SEM image of Cu nanostructured thin film grown by OAD.

Growth of nanostructured thin films using Oblique Angle Deposition (OAD) was tested in the deposition chamber of ECR plasma system. A 2 inch dia target holder was incorporated into the deposition chamber through a 6 inch CF port. Nanostructured copper films were grown by dc sputtering using argon plasma (Fig. 29). The nanostructured thin films grow due to self-shadowing regions formed during the OAD process.

4.4.9 Contact angle setup

I. Sulania, GVBS Lakshmi

The contact angle setup was not working for the past one year or so. The service engineer was called and the problem was diagnosed with the software of the setup. As the CD for software was missing a copy was obtained from the company (KRUSS, Germany) and the software was re-installed. The camera and flow rate etc were optimized by the engineer.

The system is operational now. The system was used to study (a) Au nanoparticles with PANI polymer in a composite film (having contact angle >120º) which are hydrophobic in nature and (b) Graphene films (having contact angle <50º) which are hydrophilic in nature. The images are shown in figure 30.

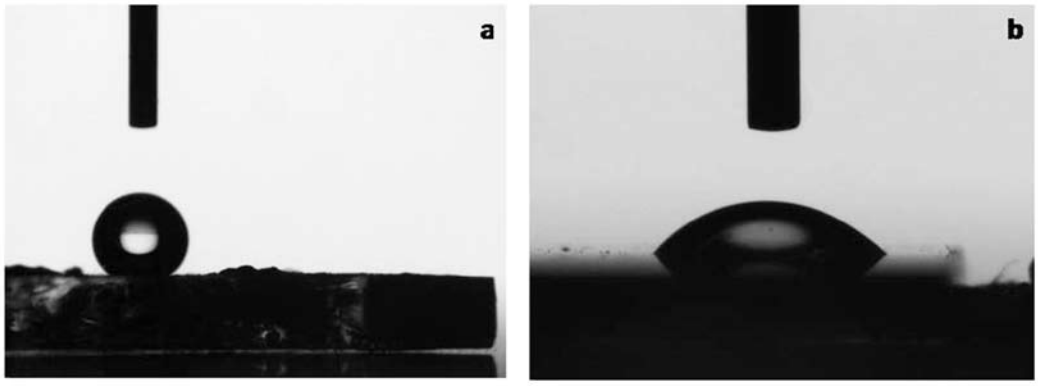

Fig. 30: (a) Contact angle image for Au and PANI nanocomposite (contact angle ~ 133º) and (b) Graphene thin films irradiated at 1×10^{11} ions/cm^2 (contact angle ~ 45º).

4.5 RADIATION BIOLOGY EXPERIMENTAL FACILITY

A. Sarma

The ASPIRE [Automated sample positioning and irradiation system for radiation biology experiments] system where irradiations of cells can be done with a set of preset doses, is being successfully utilized for different radiation biology experiments. The system is characterized by the dose uniformity over a field of 40 mm diameter within 2 % standard deviation. The mean fluence is within 1 % of the electronically measured value at the centre of the field. The characterization of the system has also been done using irradiating SSNTD [CN 85].

The radiation biology laboratory is having the following equipment to facilitate the sample preparation and post irradiation treatments.

- Two CO_2 incubators, Two biosafety cabinets, one small laminar flow bench for cell culture
- Field Inversion Gel electrophoresis, Normal gel electrophoresis, protein gel electrophoresis set up
- Image based cell counter Countess [Invitrogen] which also gives information about cell viability and Beckman-Coulter Z2 cell counter

- PCR machine, a crude gel documentation system, UV-Vis Spectrophotometer and a Fluorescence microscope.
- Perkin Elmer Multimode Plate Reader, Eppendorf and Plastocraft Refrigerated Centrifuge and a Biotek micro-plate washer.

The laboratory section has independent Split AC supply isolated from the central AC system. The CO2 supply to the twin incubators is done from outside the lab area, which facilitates the replacement of empty cylinder without disturbing the laboratory environment. Regular work is going on in the laboratory on

- Analytical procedures involving gene expression studies using PCR, Western Blot, Flurescence Immunostaining studies etc by the University Users
- Synthesis of gold nano-particles [AuNPs] of different sizes and functionalization with different agents like Glucose, Folic acid and PEG.
- Internalization of such particles by cancer cells and study of radiation interaction on them.

4.6 ATOMIC PHYSICS FACILITY

4.6.1 Progress of the Collisional spectroscopy in VUV-visible region

Gaurav Sharma[1,2], Gajendra Singh[1,2], S. K. Saini[2], R.N.Dutta[2], H.G.Berry[3], and T. Nandi[2]

[1] Dept. of Applied Physics, Delhi Technological University, Delhi 110042

[2]Inter-University Accelerator Centre, JNU New Campus, New Delhi 110067

[3]University of Notre Dame, USA

A 30 year old Mc-Pherson 225 monochromator was obtained from Notre Dame University. Unfortunately, it was not in operational condition. Last year we were in a position to work on it in convert it to a spectrometer. We decided to fix the problems of the monochromator and develop all the subsystems such as data acquisition and control using lab-view programme and calibration with Hg lamp and He-discharge lamp etc. Finally we plan to couple the spectrometer to the beam line.

Fig. 31. Spectrometer coupled with the beam line.

Synchronous motor and gear system was not functioning hence a stepper motor was installed in the Monochromator for the rotation of grating spindle. Next a non periodic play was encountered in the spindle and mechanical counter, the problem was fixed accordingly. Electro-mechanical switches were added to the spindle so that it stops the motion as soon as it approaches the ends. In order to read the precise position of grating we have installed a shaft encoder that can give us one thousand points in one turn rotation of grating spindle. This enables us to read us to the position with 0.025Å accuracy. This was controlled using a RS-232 module for recording positions of the grating in computer with DCON Utility software.

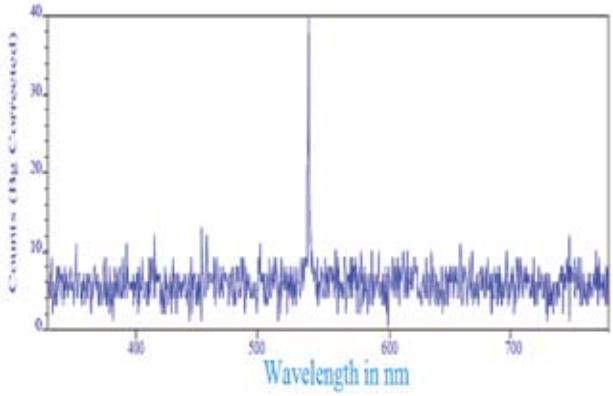

Fig 32: A small part of spectrum from of Hg lamp at 5460Å with a resolution about 1Å

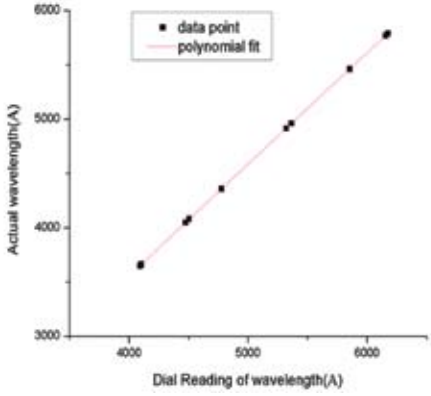

Fig 33: Wavelength calibration curve of Spectrometer

The spectra taken with Hg lamp showed broad peak of about 40Å FWHM. Reduction of vertical and horizontal slit width did not help much. In next step we put object slit, grating and exit slit on the Rowland circle and found an improvement by a factor of two. To improve further we examined that the position of focussing lens placed between wavelength shifter and CCD was fitted wrongly by manufacturer and that resulted a departure in magnification from unity. By changing the position of focussing lens we found that FWHM improved to 8Å. In order to get magnification unity the optical system required to be refabricated. Having made these major modifications we achieved expected resolution of 1Å at 5460 Å with 30micron slit size. Then the spectrometer is calibrated and the curve is shown in Fig. 33.

To make the spectrometer fully automatic we have made use of lab view programme to control all parts of the spectrometer and read them out too. Data acquisition system developed that can run the spectrometer un-attentively and thus it saves the data taking time during the experiment.

In order to calibrate our spectrometer in VUV region we developed a He discharge light source using a Penning gauge head. The source was mounted on a small vacuum chamber attached to spectrometer object side. A needle valve was used to control the He gas pressure below 1x 10-3 mbar to start up the discharge. He-plasma worked as VUV source to carry out the calibration in VUV region.

In the next step we accommodated and aligned the spectrometer in atomic physics beam line. This was indeed a difficult task we had to dismantle the charge state setup keeping an option to place it again whenever required with minimum efforts. We altered our beam line by first cutting of the supporting stand of the charge state separator device to place our spectrometer. Required bream line components including a gate valve and supporting stand were fabricated and installed successfully. Further we coupled the spectrometer with the beam line and checked the alignment using a theodalite. Now we are waiting for scheduling of allotted beam time.

4.6.2 A Setup for Experiment in the Cross-link of Atomic and Nuclear Physics

T. Nandi[1], Prashant Sharma[1], Dheeraj Chandwani[1], Gaurav Sharma1[2], Gajendra Singh[1,2], Hala[3], Haris Kunari[3], Gurpreet Kaur[4], Jagdish Gehlot[1], Akhil Jhingan[1] and Hardev Singh[5]

[1]Inter-University Accelerator Centre, JNU New Campus, New Delhi 110067

[2] Dept. of Applied Physics, Delhi Technological University, Delhi 110042

[3]Aligarh Muslim University, Aligarh 202002

[4]Panjab University, Chandigarh 160014

[5]Kurukshetra University, Kurukshetra 136119

An experiment was setup to carryout measurement in the cross-link of atomic and nuclear physics. The schematic is shown in the Fig 34. Experiments were performed in a wide range of energies starting from much below Coulomb barrier to above the barrier for different beam and target combinations at General Purpose Scattering Chamber. Well-collimated ion beam of different energies for ^{28}Si from 40-50 MeV, ^{58}Ni 41.6-156 MeV, ^{56}Fe from 40-136 MeV, ^{107}Ag from 108-120 MeV was bombarded on natural carbon of thickness 80 μg/cm^2, which was placed at 45º to the beam axis. It may be noted that natural carbon contains 99% ^{12}C and the rest ^{13}C. We plan to detect the X-rays as well as particles like α and C. Accordingly, X-rays produced in reactions were detected in two Low Energy Germanium (LEGe) detectors, placed at ±90º to the beam axis to minimize the Doppler shift and outside the chamber at 16 cm (LEGe1) and 65 cm (LEGe2) away from the target. Whereas for particle identification we made use of two different types of particle detectors, Silicon Micro-Strip Detector (MSD) and Silicon Surface Barrier Detector (SSBD) as telescope placed at ±30º to the beam axis.

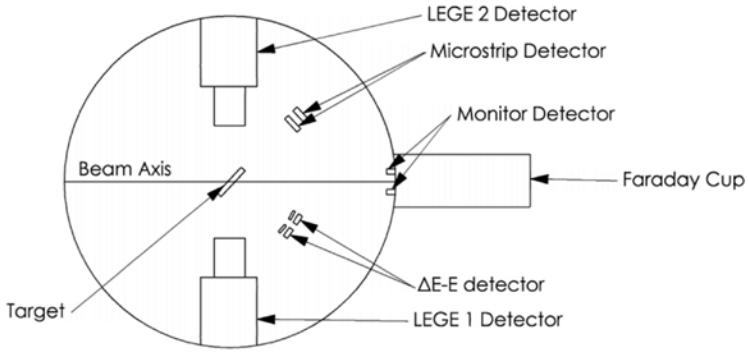

Fig 34: Schematic of experimental setup

Calibration was done for the X-ray detectors using Co-57, Fe-55 and Am-241 standard sources and resolution was found to be 3.79% for LEGe1 and 5.02% for LEGe2 at 6.41 keV. SSBD and MSD were calibrated using α-source for α peaks, whereas for ^{12}C peaks calculated ^{12}C energies from two body kinematics were used. A typical particle spectrum obtained with MSD is shown in Fig 35. It shows both α and C peaks. In this work we measured the X-ray spectra just at the time of creation i.e. at t = 0. A typical X-ray spectrum is shown in Fig 36.

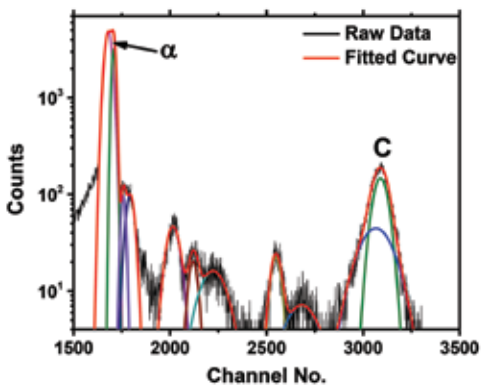

Fig 35: Particle spectrum observed in Microstrip Detector for ^{58}Ni on ^{12}C at 108 MeV

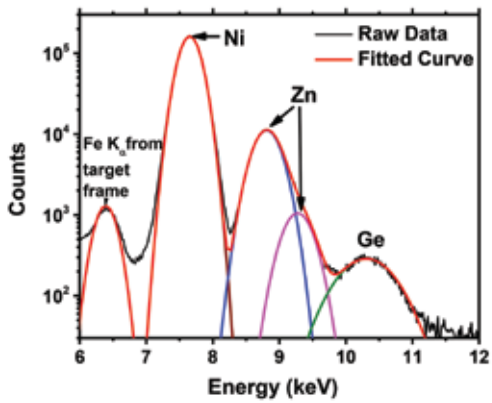

Fig 36: X-ray Spectrum observed in LEGe2 Detector for ^{58}Ni on ^{12}C at 108 MeV

Since X-ray spectroscopy provides a reliable technique to find the charge state origin during any atomic collisions [1], we compared the charge states measured at t=0 and predictions from a theoretical calculations [2]. Mean charge state of the projectile-like fragment ion is higher than that of the projectile ion. Further, the difference between theory and experiment for projectile-like ions is much larger than that for projectile ions as evident from Fig. 37. For enlightenment of this unusual outcome we have formulated a new model of electron capture from pseudo target or projectile ion described elsewhere [3].

In conclusion, the interdisciplinary program has clearly indicated new directions to studying nuclear reactions using a combination of atomic and nuclear techniques.

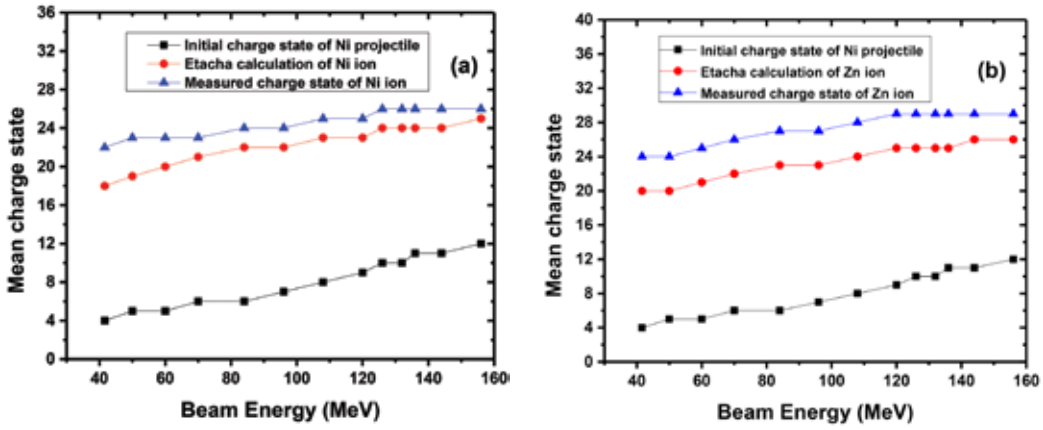

Fig. 37:Comparison between measured and theoretical mean charge state using ETACHA code for (a) Projectile ions, (b) Projectile-like ions through carbon target of equilibrium thickness

References

[1] J. P. Santos, a. M. Costa, J. P. Marques, M. C. Martins, P. Indelicato, and F. Parente, Phys. Rev. A 82, 062516 (2010).
[2] J. P. Rozet, C. Stéphan, and D. Vernhet, Nucl. Instruments Methods Phys. Res. Sect. B Beam Interact. with Mater. Atoms 107, 67 (1996).
[3] T. Nandi and P. Sharma, Annu. Rep. 5.4.3, (2014).

4.7 ACCELERATOR MASS SPECTROMETRY

Pankaj Kumar, Rajveer Sharma, Sunil Ojha, S. Gargari, R. Joshi, G.S. Roonwal and S.Chopra

Accelerator Mass Spectrometry (AMS) facility for ^{10}Be and ^{26}Al measurement is in operation using 15UD Pelletron Accelerator. A new facility is being set up for ^{14}C AMS measurements. The clean chemistry laboratory is extensively utilized by various users for the chemical treatment and extraction of ^{10}Be and ^{26}Al from their samples. A brief of the activities performed in last year are explained below:

4.7.1 Enhancing BeO- beam current by co precipitating Nb with BeO:

Sensitivity and accuracy of ^{10}Be AMS measurement depends upon the generation of negative ion current from ion source. Higher is the ion current from source, better is the ^{10}Be statistics. To enhance thermal and electrical conductivity BeO powder is mixed with Nb/Ag/ Cu metal powder before loading into the ion source. Powder-powder mixing of metal powder in BeO has several laboratory handling drawbacks. First of all it involves grinding and mixing which is a time consuming process. Also BeO dust is a carcinogenic, if it releases during grinding, it may cause serious health risk. During pressing of this mixture (BeO and metal powder) into a cathode, beryllium oxide has a tendency to get a steady charge which may lead to loss of sample material. Co-precipitation of beryllium with niobium or silver is able to remove above laboratory handling difficulties. We explored the co-precipitation technique using various Nb:Be ratios at IUAC-AMS facility.

Various amounts of Nb solution was added to the BeO solution [Be(OH)2] and following ratio of Nb:Be by weight: 0.7:1, 1.3:1, 2:1, 3.3:1, 4.7:1, 6:1, 7.3:1, 8.6:1, 10:1, 13.3:1 were obtained. For co-precipitation, few drops of NH3 were added to maintain pH of solution at 10. Precipitations were washed three times with MQ water and centrifuged for 5 minutes at 3000 rpm. Precipitations were transferred into quartz vials and heated upto 800°C for 8 hrs for converting into BeO form. Samples thus prepared were loaded into cathode tube and tested in the ion source. Analysed current for mass 25 ($^{9}Be^{16}O$) is plotted against time in fig. 38.

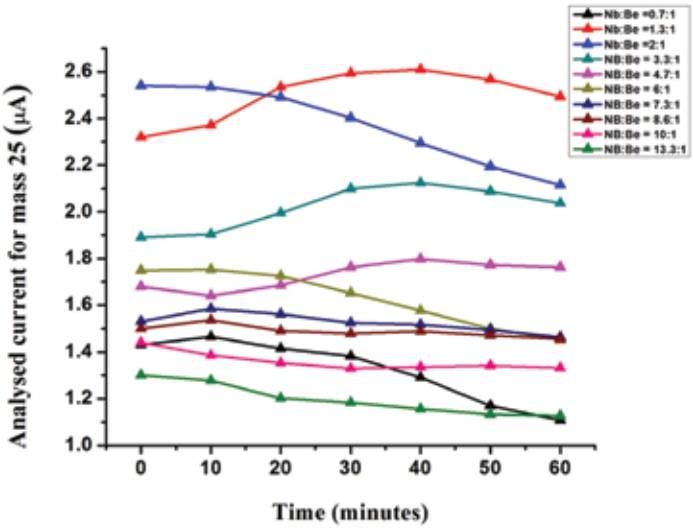

Fig: 38: Analysed mass 25 ($^{9}BeO^{-}$) current from ion source with respect to sputtering time

It is evident from fig. 38 that higher amount of Nb metal does not necessarily lead in producing high current. The maximum current observed was 2.68 micro amperes for the ratio 1.3:1 after 20 minutes of sputtering. For initial 20 minutes, maximum current of 2.53 microamperes was obtained for the ratio 2:1. Detailed co-precipitated study using other metal matrices and their comparison to powder-powder mixing is in progress.

4.7.2 ^{14}C AMS facility

A new AMS facility based on dedicated 500kV ion accelerator is being established at IUAC. In addition to the ^{14}C measurements, the proposed system can perform ^{10}Be and ^{26}Al measurements

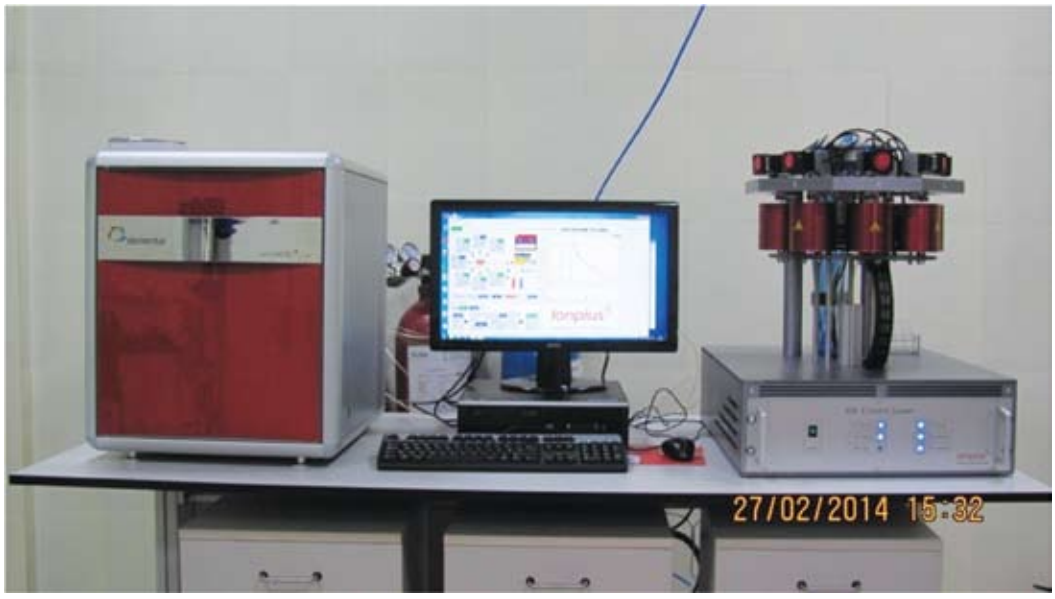

Fig. 39: Automated Graphitization Equipment installed in graphitization laboratory at IUAC

also with better precision than using existing 15UD Pelletron accelerator. The facility shall be operational by the December 2014.

For ^{14}C measurements, samples need to be converted in graphite form. CO_2 is extracted from samples by combustion, purified and converted into elemental carbon by graphitization. An automated graphitization equipment (AGE) has been developed in collaboration with ETH, Zurich [Fig. 39]. A laboratory for samples pretreatment and graphitization has also been developed at IUAC.

Automated graphitization equipment (AGE) contains two units; first is the elemental analyser and other is graphitization system. Pretreated samples are wrapped in a tin capsule and dropped inside elemental analyser for combustion in the presence of oxygen gas. After combustion CO_2 is produced and trapped in zeolite trap inside the elemental analyser. At certain temperature CO_2 is released from trap and transferred to the reactor (Fe powder containing glass tube) of graphitization unit. Finally, the hydrogen is added to reactor in the ratio of 2.3:1 (H_2: CO_2). For graphitization reactors are heated to 580°C and CO_2 starts reacting with H_2 following the reaction:

CO_2+ 2H_2→ C+ 2H_2O (In the presence of Fe as catalyst)

The H_2O produced in the reaction is condensed by Peltier coolers mounted on the top of reactors. All the steps in the graphitization unit are logged, displayed and controlled using LabVIEW interface.